Back to Norway

An Essay

Kerry Emanuel[1]

Program in Atmospheres, Oceans, and Climate

Massachusetts Institute of Technology

Cambridge, MA 02139

Submitted 23 May 2005

Revised

9 April 2006

[1] *Corresponding author address*: Rm. 54-1620, MIT, 77 Massachusetts Avenue, Cambridge, MA 02139 Email: emanuel@texmex.mit.edu

Abstract

The advent of the polar front theory of cyclones in Norway early in the last century held that the development of fronts and air masses is central to understanding middle latitude weather phenomena. While work on fronts continues to this day, the concept of air masses has been largely forgotten, superseded by the idea of a continuum. The Norwegians placed equal emphasis on the thermodynamics of air mass formation and on the dynamical processes that moved air masses around; today, almost all the emphasis is on dynamics, with little published literature on diabatic processes acting on a large scale. In this essay, I argue that lack of understanding of large-scale diabatic processes leads to an incomplete picture of the atmosphere and contributes to systematic errors in medium- and long-range weather forecasts. At the same time, modern concepts centered around potential vorticity conservation and inversion lead one to a re-definition of the term “air mass” that may have some utility in conceptualizing atmospheric physics and in weather forecasting.

1. Introduction

Fronts and air masses are generally regarded as the two key concepts that emerged from the "Norwegian School", founded by Vilhelm Bjerknes and carried on by his son, Jacob, together with Tor Bergeron, Halvor Solberg, Erik Palmén, and others. Fronts were considered to be boundaries between air masses with distinct thermodynamic properties. According to Bergeron (1928),

> *An air mass is a vast body of air whose physical properties are more or less uniform in the horizontal, while abrupt changes are found along its boundaries, i.e. the frontal zones.*

The Norwegians envisioned an intimate relationship among fronts, air masses and cyclones:

> *The cyclone consists of two essentially different air-masses, the one of cold and the other of warm origin. They are separated by a fairly distinct boundary surface which runs through the center of the cyclone. This boundary surface is imagined to continue, more or less distinctly, through the greater part of the troposphere* (Bjerknes and Solberg, 1922)

Note that the frontal boundary separating air masses was thought to run through the whole depth of the troposphere. This idea was later discredited by Sanders (1955), who showed, using surface and upper air data, that fronts are generally very shallow features, rarely detectable more than a kilometer or two above the surface. Still later, Hoskins and Bretherton (1972) demonstrated on theoretical grounds that true fronts, defined as near discontinuities in long-front velocity, can only form at rigid boundaries or at pre-existing discontinuities in the distribution of potential vorticity, such as the tropopause. But I shall argue later in this essay that deep fronts may indeed occur along the equatorward boundary of arctic air masses.

The Norwegians placed a great deal of emphasis on air mass formation. They defined essentially four air masses, based on whether they were of continental or maritime origin, and whether they were warm or cold. Although they recognized the influence of radiative processes in the atmosphere itself, they clearly regarded the underlying surface as the basic progenitor of air masses, largely defining their properties. Bergeron visualized air masses as forming within semi-permanent circulation systems, such as wintertime continental highs and subtropical anticyclones:

> *The air that takes part in the circulation around any such system will become subject to the prolonged influences of the underlying surface, with the result that there will be a tendency for distinct properties to be acquired. Although the vertical structure of any air mass may be modified by differential advection and vertical stretching and shrinking, the more direct modifications are brought about by interactions between the atmosphere and the earth's surface.* (Bergeron, 1922, as paraphrased by Petterssen (1956))

Air masses were characterized not only by their surface properties but, in particular, by their vertical structure as revealed by radiosondes. Arctic air masses were characterized as having very stable temperature profiles in the lowest layers, while, for example, maritime tropical air was revealed by deep layers of moist adiabatic lapse rates. The thermodynamics of air mass formation were studied in detail and were regarded on an equal footing as the dynamical processes that moved air masses around.

Then came the dynamics revolution, fostered by the theory of baroclinic instability developed by Charney (1947) and Eady (1949), and the subsequent development of quasi-geostrophic theory by Charney and Phillips (e.g. Charney and Phillips, 1953) and others. In the ensuing firestorm of progress in dynamical theory and in numerical weather prediction, thermodynamics took a back seat. In many beginning courses in atmospheric dynamics, thermodynamics is often developed only so far as

demonstrating the conservation of potential temperature. Although Eady, in his 1949 paper, emphasized the central role of latent heat release in the dynamics of extratropical cyclones, it took another quarter century for theorists to take much interest in this issue, and today, the phrase “diabatic processes” is virtually synonymous with “latent heat release”. Although it is recognized that radiative processes must be included in numerical weather prediction models, they are regarded by forecasters as operating on a long time scale or as influencing only the boundary layer on diurnal time scales. Almost all contemporary discussions of weather prediction and predictability focus on dynamical error growth, with some attention paid to the incorrect representation of convection and almost none to radiative processes. Meanwhile, the term “air mass” has been shelved together with such antiquities as “polar front” and “weather breeder”.

The contemporary view of the physics of fronts and cyclones can be traced back to the work of Ernst Kleinschmidt, Eric Eady, Jule Charney, Brian Hoskins and Francis Bretherton. This view may be broadly summarized as follows:

- The baroclinic dynamics of quasi-balanced systems outside the Tropics (and to some extent within them) may be thought of in terms of the conservation and invertibility of potential vorticity
- Isentropic gradients of potential vorticity, which serve as the conduits of Rossby waves, are concentrated at the tropopause and, effectively, at the surface where there is a strong temperature gradient.
- The troposphere itself may be thought of as a region of constant potential vorticity, or nearly constant potential vorticity gradient.
- Most of the dynamics of extratropical weather systems may be conceptualized in terms of the propagation and interaction of Rossby waves at the tropopause and

surface, and to a lesser extent, in the tropospheric continuum, perhaps modified by latent heat release

- Fronts are features of the surface and (deformed) tropopause
- 5-10 day forecast errors are owing to dynamical error growth; sensitivity can be approximately measured by adiabatic error growth

With the exception of the important distinction between the troposphere and stratosphere, the concept of air masses is entirely missing from this point of view, as is any accounting for radiative effects. The author has taught an advanced graduate course in quasi-balanced dynamics at MIT for 15 years and very much subscribes to the view described briefly above. But there are times and places where being conscious of radiative processes seems necessary for understanding the medium range evolution of the atmosphere, while there may be some utility in re-introducing the concept of air masses, albeit with a contemporary spin.

2. Evolution of arctic air

The formation of cold air, by radiative cooling, is problematic. Most of the cooling is at the surface itself, and as the air adjacent to the surface cools, the air mass becomes increasingly stable and impervious to vertical mixing. Aside from weak radiative cooling in the interior, there is no mechanism for propagating the surface cooling upward to affect a deep layer. (The same problem occurs upside down in the ocean, where vertical mixing is the only way to propagate surface warming down into the interior (Sandstrom, 1908; Jeffreys, 1925).)

In what I view as a landmark paper, Judith Curry drew attention to the peculiar thermodynamics involved in the formation of continental arctic air masses (Curry, 1983).

She noted that time series of atmospheric soundings, such as repeated here in Figure 1, show cooling through the first few kilometers of the atmosphere at rates that exceed those one might expect based on simple radiative models. Figure 1 shows a sequence of soundings from Fairbanks, Alaska, in December. Even 1 km above the surface, the air cools about 30^{o}C over the course of two weeks. Of course, some of this might be by advection, but examination of re-analysis data over the Canadian arctic during winter shows the minimum temperature in an isolated pool of cold air can fall many degrees in a week; this is almost certainly the effect of radiative cooling.

Curry pointed out that the rate of cooling is sensitive to the moisture content of the air, the presence or absence of condensed water (ice crystals, at these temperatures), and the rate of subsidence. Curry began by using a radiative transfer code to calculate the evolution of temperature in a single column, beginning with a dry, nearly moist adiabatic profile with a surface temperature of 0^{o}C. I repeat these calculations here using a different radiative code and starting with a tropical sounding, but removing most of the water vapor so that clouds do not form. (The code uses the radiation scheme of Morcrette (1991), the convection scheme of Emanuel and Živkovic-Rothman (1999), and the fractional cloudiness scheme of Bony and Emanuel (2001).) As Figure 2 shows, the air cools down very rapidly at the surface, but even at 600 hPa the rate of cooling is large enough to be of concern even for a short range forecast. If we re-run this calculation but starting from a reasonable moisture profile and allow clouds to develop, the column cools much less rapidly, owing both to latent heat release and to the insulating effect of clouds. A more interesting calculation is to assume that large-scale subsidence has dried out the column, except near the surface, and allow clouds to develop only in the boundary layer as the air cools. The results of one such calculation are shown in Figure 3. Clouds form in the boundary layer, which deepens with time

owing to the bootstrapping mechanism identified by Curry: Radiative cooling at the cloud top leads to condensation there, which deepens the existing cloud. But as the cloud thickens, this cooling becomes large enough that the boundary layer is destabilized, resulting in convective mixing, which dries the cloud and causes it to break up. (The interested reader should consult Curry (1983), who used a more physically correct representation of ice crystals than the model shown here.)

As Curry recognized, these calculations are not very realistic because they omit the large-scale subsidence that almost certainly accompanies the formation of arctic air. With a single column, it is not possible to directly calculate the subsidence, which requires 2-D or 3-D dynamics, but one can get a rough feeling for the effects of subsidence by simply specifying a vertical subsidence profile. Here we specify a smooth profile of subsidence, vanishing at the surface and at 100 hPa and reaching a peak value of 0.5 hPa hr^{-1} at 750 hPa. To allow condensation to occur in the boundary layer in this calculation, we increase the initial amount of moisture in the lower troposphere. As shown in Figure 4, the boundary layer grows owing to cloud top cooling, but slowly asymptotes to an equilibrium height of about 750 hPa, at which point this deepening effect is balanced by subsidence. Not only does the cold boundary layer become substantially deeper, but the air above the boundary layer cools somewhat faster than it did in the clear case, perhaps owing to larger concentrations of water vapor in this simulation. Another interesting feature of this simulation is the development of a new low-level inversion, separating two nearly dry adiabatic layers, at day 30.

While calculations such as Curry's and those presented here cannot be regarded as precise simulations of the formation of arctic air, they do illustrate that the time scale of and depth through which radiative cooling acts are sensitive to the water vapor

content of the air mass and the presence of clouds, as well as to the magnitude of the large-scale subsidence. Given that the absolute amounts of water involved are very small, and that some of its sources, such as sublimation of snow, may be difficult to model, it is questionable whether today's forecast models are capable of accurate simulation of arctic air mass formation on ten-day time scales.

3. A Revised Air Mass Classification

The general idea of an "air mass" is something that once formed tends to preserve its thermodynamic properties as it is advected around. The Norwegians classified air masses based mostly on the nature of vertical temperature profiles and on moisture content. Here we propose a new classification based on a single quasi-conservative variable, the *saturation potential vorticity*, hereafter, the "*SPV*":

$$SPV \equiv \rho^{-1}\left[2\mathbf{\Omega} + \nabla \times \mathbf{V}\right] \bullet \nabla \ln \theta_e^*, \tag{1}$$

where ρ is the air density, $\mathbf{\Omega}$ the earth's angular velocity vector, $\mathbf{V}$ the fluid velocity vector, and θ_e^* the saturation value of the equivalent potential temperature. (I prefer to use the natural log of θ_e^* because it is then proportional to the entropy.) *SPV* has several very nice characteristics:

- It is *always invertible*, provided the flow is balanced, since θ_e^* is a state variable.
- It is nearly conserved in very cold air (e.g. arctic air, stratospheric air), because in the cold limit it reduces to the ordinary potential vorticity (*PV*), since $\theta_e^* \to \theta$ at low temperature.

- Neutrality to (slantwise) convection is characterized by $SPV = 0$, which is equivalent to having moist adiabatic lapse rates along vortex lines (absolute momentum surfaces, in two dimensions). Thus in much of the tropical and middle latitude free troposphere, where we observe convective neutrality (Emanuel, 1988; Xu and Emanuel, 1989), *SPV* is nearly zero.

Note that although *SPV* is not materially conserved, it is nearly so in cold air, and in convectively adjusted air it is zero, which is just as good as being conserved[2].

Based on these characteristics, I define four air masses:

Convected: *SPV=0*. (Moist adiabatic lapse rates on vortex lines.) Formation time of 1-2 days. Most of the troposphere, most of the time.

Stratosphere: High *SPV* reservoir. Long formation time scales. $SPV \cong PV$ owing to low temperatures.

Arctic: High *SPV* owing to radiative cooling in continental interior in winter. Formation time of 4-14 days.

PBL (planetary boundary layer)**:** Over much of ocean and land during daytime, $SPV < 0$ owing to dry adiabatic (e.g. super-moist adiabatic) lapse rates. Over cold water and at night over land, SPV may become positive. Formation time of 1-12 hours.

[2] Note that unlike in the case of classical *PV*, all the terms in (1) must be used in calculating *SPV*; one may not approximate it as the product of the vertical component of vorticity with the vertical gradient of $\ln \theta_e^*$. This is because the latter is typically much less than the vertical gradient of $\ln \theta$.

An example of a cross-section of *SPV* is shown in Figure 5; this is taken along 90^{o}W at 00 GMT on 8 March 2003. I have subjectively delineated the boundaries between arctic, stratospheric and convected air. Note that much of the tropical and middle latitude troposphere has $SPV \simeq 0$, and that the boundary between the troposphere and stratosphere is usually well delineated, as in the case of *PV*. The transition zone between convected and arctic air lies between about 30^{o}N and 45^{o}N in the section. The actual values of *SPV* in convected and stratospheric air are well defined by convective and radiative equilibrium, respectively, but as noted is section 2 above, the thermodynamic profiles (and therefore *SPV*) are highly variable in arctic air, owing to its sensitive dependence on clouds, water vapor and subsidence. There is little evidence of PBL air in this section, perhaps because of the low vertical resolution of the re-analysis data used to construct the section.

In summer, arctic air, if it can be said to exist at all, has smaller values of *SPV* and can only be found at very high latitudes, as illustrated in Figure 6, which shows a cross-section along 100^{o}W at 00 GMT 7 July 2003. Arctic air can only be found poleward of 70^{o}N, and its *SPV* is smaller than in the winter section of Figure 5. The local patches of relatively high SPV near the tropopause and around 50^{o}N may be real, but they are perhaps artifacts of the model used for the re-analysis.

Note that much of the troposphere often has $SPV \simeq 0$ even though very little of it is convecting at any one time. Convection is a comparatively fast process and where and when it occurs, it establishes nearly moist adiabatic lapse rates in a matter of hours (perhaps a little longer when the convection is slantwise). But once the convection ceases, it takes radiation and/or subsidence much longer to pull the lapse rates away from moist adiabatic (except in the PBL). A convecting air column over the North Pacific

in winter may only take a few days to cross the North American continent, which may not be long enough to change its *SPV* appreciably.

From the perspective of *SPV* inversion (remember that *SPV* can be inverted just like *PV*, provided a balance approximation is valid), to a first approximation, one only needs to know the distributions of *SPV* in the artic air and the stratosphere, the distribution of θ_e^* at the top of the boundary layer, and the topology of the boundaries separating the stratospheric, convected, and artic air masses. This suggests a basis for a stripped down, quasi-balanced model integrating only the surface θ_e^*, the tropopause, and the boundary between arctic and convected air. I present one very simple example of this in the next section.

4. The Arctic Front

The Norwegians talked about a “polar front” separating polar from tropical air, and they believed that it extended from the surface to the tropopause. Later observational (Reed and Sanders, 1953; Reed, 1955; Sanders, 1955) and theoretical (Hoskins and Bretherton, 1972) work established that true fronts (i.e. near discontinuities in long-front velocity and cross-front temperature gradient) can only form at the surface and at pre-existing regions of sharp *PV* gradients, such as the tropopause. Almost all of the current literature on atmospheric fronts refers to surface and tropopause fronts; the latter, of course, may extend downward even to the lower troposphere. There is a small literature on arctic fronts, and Peter Hobbs and co-workers (e.g. Wang et al., 1995) have recognized that these can be quite deep, with regions of strong horizontal temperature contrast extending through much of the troposphere, together with frontogenetical forcing.

The transition between arctic air of high *SPV* and convected air with *SPV* = 0 may extend through most or all of the troposphere, as shown in Figure 5. In principle, deep geostrophic deformation acting on this transition is capable of forming a front extending through the troposphere, much as the Norwegians had imagined. To illustrate this point, we develop a simple, analytic, semi-geostrophic model of frontogenesis that closely follows that of Hoskins and Bretherton (1972). The semi-geostrophic equations are the geostrophic momentum equations phrased in geostrophic coordinates. For fronts aligned (arbitrarily) along the *y* axis, and using the Boussinesq, *f*-plane version of the geostrophic momentum equations, the appropriate horizontal, cross-front geostrophic coordinate, *X*, is defined

$$X \equiv x + \frac{v_g'}{f}, \tag{2}$$

where x is the physical cross-front coordinate and v_g' is the departure of the meridional component of the geostrophic wind from the background deformation. We assume, as did Hoskins and Bretherton, that on the time scale of front formation, the flow is adiabatic and inviscid, so that both potential temperature and *PV* are conserved. Conservation of *PV* can be expressed in geostrophic coordinates as

$$\frac{\partial PV}{\partial \tau} + \frac{dX}{dt}\frac{\partial PV}{\partial X} + w\frac{\partial PV}{\partial Z} = 0, \tag{3}$$

where $\frac{\partial}{\partial \tau}$ is the time derivative holding altitude and X constant, and likewise $\frac{\partial}{\partial Z}$ is the derivative in height holding time and X constant. Given the distribution of *PV* at any time, the distribution of potential temperature can be found by inverting the *PV* distribution via

$$\frac{\partial^2\theta}{\partial X^2}+\frac{f^3}{g}\frac{\partial}{\partial Z}\left[\frac{1}{PV}\frac{\partial\theta}{\partial Z}\right]=0, \tag{4}$$

subject to the time-dependent boundary conditions

$$\frac{\partial\theta}{\partial\tau}+\frac{dX}{dt}\frac{\partial\theta}{\partial X}=0 \tag{5}$$

on rigid horizontal boundaries (on which *w* vanishes). The cross-front circulation as represented by a streamfunction, ψ, may be diagnosed from a Sawyer-Eliassen type equation, which phrased in geostrophic coordinates, is

$$\frac{\partial}{\partial X}\left(\frac{PV}{f}\frac{\partial\psi}{\partial X}\right)+\frac{\partial}{\partial Z}\left(\frac{f^2}{g}\frac{\partial\psi}{\partial Z}\right)=Q, \tag{6}$$

where Q is the geostrophic forcing, which is proportional to the product of the geostrophic deformation and the cross-front temperature gradient.

As in Hoskins and Bretherton, we shall consider an idealized, height-independent deformative geostrophic flow given by

$$u_g=-\alpha x, \qquad v_g=\alpha y, \tag{7}$$

where α is the rate of deformation. Owing to symmetry, the deformative part of the geostrophic flow remains constant in time in this problem. Hoskins and Bretherton show that for this flow,

$$\frac{dX}{dt}=-\alpha X. \tag{8}$$

In this application, I start with an initial potential vorticity field that is a function of X alone. Since the geostrophic flow in the *x* direction does not vary with height, one can see from (3) that *PV* will never acquire a *Z* dependence, so that (3) reduces in this case to

$$\frac{\partial PV}{\partial \tau} - \alpha X \frac{\partial PV}{\partial X} = 0, \tag{9}$$

where I have used (8). Equation (9) has a simple analytic solution:

$$PV = F\left(Xe^{\alpha\tau} \right), \tag{10}$$

where $F(X)$ is simply the initial *PV* distribution. As Hoskins and Bretherton point out, time becomes a parameter in this problem. Likewise, the boundary condition for θ (5) becomes

$$\frac{\partial \theta}{\partial \tau} - \alpha X \frac{\partial \theta}{\partial X} = 0 \tag{11}$$

which similarly has the solution

$$\theta = G\left(Xe^{\alpha\tau} \right), \tag{12}$$

where $G(X)$ is the initial distribution of θ. (A similar condition applies at each boundary.) For simplicity, we take the tropopause here to be a rigid boundary. The geostrophic forcing function Q in (6) becomes, in this case

$$Q = -2\alpha \frac{\partial \theta}{\partial X}. \tag{13}$$

Thus given the initial one-dimensional distributions of *PV* and boundary θ, we immediately have the distributions of these quantities in geostrophic space for all time, from (10) and (12). We can then invert (4) for the interior θ distribution, and (6) and (13) for the streamfunction ψ.

An interesting special case is one in which θ is constant on the upper boundary. We also take the initial lower boundary θ and interior *PV* both to follow hyperbolic tangent functions, so that they have no gradients as $X \to \pm\infty$. The solution for various quantities at about the time of surface frontal collapse is shown in Figures 7. Note that

the *PV* itself has formed a front at the surface, and that even though there is no temperature gradient along the tropopause in this case, local extrema of vorticity form there. Both the vorticity and upward vertical motion extend deeper into the troposphere than in the uniform potential vorticity case.

An example of an arctic front as it appears at the 500 hPa level at 18 GMT on 6 January, 2004, is shown in Figure 8. A ribbon of high vorticity extends from the central plains across western Pennsylvania and New York State, through northern New England and the Canadian Maritimes. There was little evidence of a wind shift at the surface, and the only weather possibly associated with this feature were some scattered light snow showers in New England. The wind profiler at Gray, Maine, recorded a wind shift in the altitude range of 500 m to 2 km, from west to northwest, sometime between 1100 and 1200 GMT. (The profiler observations did not penetrate above 2 km in the arctic air.)

Clearly, arctic air may develop significant *PV* gradients at its leading edge, and these may lead to some interesting dynamics not captured by analysis techniques that focus on the surface and the tropopause. Dynamics associated with arctic air are ripe for more comprehensive analysis.

5. Summary

The Norwegian school of meteorology placed roughly equal emphasis on the importance of dynamics and thermodynamics for understanding and forecasting weather. They viewed the development of fronts as being largely a dynamical phenomenon, but they were equally concerned with the thermodynamics of air mass formation. Today, understanding and predicting weather at short to medium range is viewed mostly as a dynamical problem, with some attention paid to surface fluxes and

latent heat release, and the idea of air mass formation has gone the way of Edsels and argyle socks. Of course, weather forecast models include processes such as surface fluxes and radiative transfer that the Norwegians considered essential to air mass formation, and much attention is paid to the representation of moist convection, which is critical to the formation of what we here call “convected air”. While it is not likely that today’s models are making first-order errors in the modification of air masses that are heated from below, which entails the relatively fast and efficient process of convection, not so much attention is paid to the problem of cooling from below, which is far more problematic. The work of Curry (1983), reviewed here, suggests that radiative cooling over land in winter may sometimes affect deep layers on time scales of ten days, depending perhaps delicately on such matters as moisture content and the microphysics of ice crystals and their interaction with radiation. I have the impression that medium range forecasts of what we often refer to as “arctic air outbreaks” are often compromised by incomplete representations of these physical processes, whereas map discussions almost always focus on the dynamics. The thermodynamics of arctic air is an area ripe for research advances.

The dynamics revolution of the late 1940s did away with the Norwegian concept of air masses and replaced it with the idea of a continuous distribution of properties, modulated by baroclinic wave and frontal processes. But “potential vorticity thinking”, advocated, for example, by Hoskins et al. (Hoskins et al., 1985) and widely employed in graduate level instruction, in effect re-introduced the concept of air masses in a new guise: tropospheric air with low but nearly constant *PV*, and stratospheric air, with much larger values of *PV*. Our current concept of extratropical dynamics holds that what we see on weather maps can be explained by the interaction of two Rossby wave trains: one on the surface temperature gradient, and another on the isentropic gradients of *PV*

at the tropopause, where isentropes cross *PV* contours. (This tropopause zone of intersection is often very narrow, horizontally, giving rise to what might be called “Rossby wave highways”.) We supplement this basic view by accounting for *PV* created by latent heating, and for the effects of surface friction.

Soundings in the Tropics, over land in the summer, and over water in the winter often show nearly moist adiabatic structure, though in strongly baroclinic regions one observes moist adiabatic lapse rates on vortex lines (*M* surfaces) rather than in the vertical. Based on this observation, together with the clear utility of PV thinking, I advocate a re-classification of air masses based on the value of a single scalar variable: the saturation potential vorticity (*SPV*), defined by (1). This quantity is zero wherever the lapse rate is moist adiabatic on vortex lines (which are nearly vertical in the Tropics), but is large in the stratosphere and in arctic air. It is nearly conserved in cold air, where it is nearly equal to conventional *PV*, and although not conserved in unsaturated warm air, it there tends to be adjusted to near zero by convection. Like *PV*, it is always invertible, subject to a balance condition. Cross-sections, such as that shown in Figure 5, suggest that the global atmosphere may be approximately described in terms of three or four air masses. “*SPV* thinking” would proceed along much the same lines as “*PV* thinking”, but replacing surface temperature with surface θ_e, which in convected air is linked to θ_e^* above the boundary layer by the condition of convective neutrality. It would also be concerned with the diabatic formation of arctic air, and the dynamics of the *SPV* transition between arctic and convected air.

Perhaps it is time to bring back the air masses.

Acknowledgements: I am indebted to Dave Schultz for helping me with the analysis of the 8 March 2003 arctic air outbreak in the central U.S., and to Rob Korty for writing the programs used to construct the *SPV* cross-sections. The manuscript was much improved by the suggestions of several anonymous reviewers.

Fred Sanders befriended me when I entered MIT as a freshman in 1973, and has been my friend and mentor ever since. Among the many priceless lessons I have learned from him was to revere our scientific forebears, even while retaining a healthy skepticism of their work.

References

Bergeron, T., 1928: Über die dreidimensional verknüpfende Wetteranalysee. *Geofys. Publ.*, **5** (6), 1-111

Bjerknes, J. and H. Solberg, 1922: Life cycles of cyclones and the polar front theory of atmospheric circulations. *Geofys. Publ.*, **3**, 1-18

Bony, S. and K. A. Emanuel, 2001: A parameterization of the cloudiness associated with cumulus convection: evaluation using TOGA COARE data. *J. Atmos. Sci.*, **58**, 3158-3183

Charney, J. G., 1947: The dynamics of long waves in a westerly baroclinic current. *J. Meteor.*, **4**, 135-163

Charney, J. G. and N. A. Phillips, 1953: Numerical integration of the quasi-geostrophic equations for barotropic and simple baroclinic flows. *J. Atmos. Sci.*, **10**, 71-99

Curry, J., 1983: On the formation of continental polar air. *J. Atmos. Sci.*, **40**, 2278-2292

Eady, E. T., 1949: Long waves and cyclone waves. *Tellus*, **1**, 33-52

Emanuel, K. A., 1988: Observational evidence of slantwise convective adjustment. *Mon. Wea. Rev.*, **116**, 1805-1816.

Emanuel, K. A. and M. Živkovic-Rothman, 1999: Development and evaluation of a convection scheme for use in climate models. *J. Atmos. Sci.*, **56**, 1766-1782

Hoskins, B. J. and F. P. Bretherton, 1972: Atmospheric frontogenesis models: Mathematical formulation and solution. *J. Atmos. Sci.*, **29**, 11-37

Hoskins, B. J., M. E. McIntyre and A. W. Robertson, 1985: On the use and significance of isentropic potential vorticity maps. *Quart. J. Roy. Meteor. Soc.*, **111**, 877-946

Jeffreys, H., 1925: On fluid motions produced by differences of temperature and humidity. *Quart. J. Roy. Meteor. Soc.*, **51**, 347-356

Morcrette, J.-J., 1991: Radiation and cloud radiative properties in the European Centre for Medium-Range Weather Forecasts forecasting system. *J. Geophys. Res.*, **96**, 9121-9132

Petterssen, S., 1956: *Weather Analysis and Forecasting: Vol. 1: Motion and Motion Systems*. 2nd *ed,* McGraw-Hill, New York, 428 pp

Reed, R. J., 1955: A study of a characteristic type of upper-level frontogenesis. *J. Meteor.*, **12**, 226-237

Reed, R. J. and F. Sanders, 1953: An investigation of the development of a mid-tropospheric frontal zone and its associated vorticity field. *J. Meteor.*, **10**, 338-349

Sanders, F., 1955: An investigation of the structure and dynamics of an intense surface frontal zone. *J. Atmos. Sci.*, **12** , 542-552

Sandstrom, J. W., 1908: Dynamische Versuche mit Meerwasser. *Annals in hydrodynamic marine meteorology*, p.6

Wang, P.-Y., J. E. Martin, J. D. Locatelli and P. V. Hobbs, 1995: Structure and evolution of winter cyclones in the central United States and their effects on the distribution of precipitation. Part II: Arctic fronts. *Mon. Wea. Rev.*, **123**, 1328-1344

Xu, K.-M. and a. K. A. Emanuel, 1989: Is the tropical atmosphere conditionally unstable? *Mon. Wea. Rev.*, **117**, 1471-1479.

Figure Captions

1. Successive temperature soundings at Fairbanks, Alaska, in December, 1961. Curves labeled with time in days relative to first sounding. After Curry (1983).

2. Evolution of the vertical profile of temperature in a single-column radiative-convective model, beginning with a tropical sounding with 99% of the water vapor removed at each level. Profile labeled in days relative to the initial sounding. Model described in text.

3a: Evolution of the vertical profile of temperature in a single-column radiative-convective model, beginning with a tropical sounding. In this case, the fraction of water removed increases from 90% at the surface to 99% at 100 hPa.

3b: Time-height plot of the fractional cloudiness in the simulation described in Figure 3a.

4. Evolution of the vertical profile of temperature in a single-column radiative-convective model, beginning with a tropical sounding. In this case, the fraction of water removed increases from 60% at the surface to 99% at 100 hPa. A smooth vertical profile of ω is specified, vanishing at the surface and at 100 hPa and reaching a peak value of 0.5 hPa hr^{-1} at 750 hPa.

5. Cross-section of saturation potential vorticity (*SPV*) along 90^{o}W at 00 GMT on 8 March 2003. Value have been multiplied by 10^4, and all values larger than 2×10^4 have been reset to 2×10^4. The three main air masses are identified.

6. Cross-section of saturation potential vorticity (*SPV*) along 100^{o}W at 00 GMT 7 July 2003. Value have been multiplied by 10^4, and all values larger than 2×10^4 have been reset to 2×10^4.

7. Solutions of the semi-geostrophic model of frontogenesis produced by uniform geostrophic deformation acting on initial hyperbolic tangent profiles of potential vorticity and surface potential temperature. (In this simulation, the potential temperature along the top boundary is constant.) The PV does not vary with altitude in geostrophic coordinates. Solutions are shown at about the time of surface frontal collapse.
a) Potential temperature; b) Long-front wind component (ms^{-1}); c) Vertical component of relative vorticity (10^{-5} s^{-1}); d) Potential vorticity (standard *PV* units); e) Mass streamfunction; f) vertical velocity (cm s^{-1}).

8. 500 hPa analysis at 1800 GMT 6 January 2004, showing geopotential height (contours) and vertical component of geostrophic absolute vorticity (yellow shading).

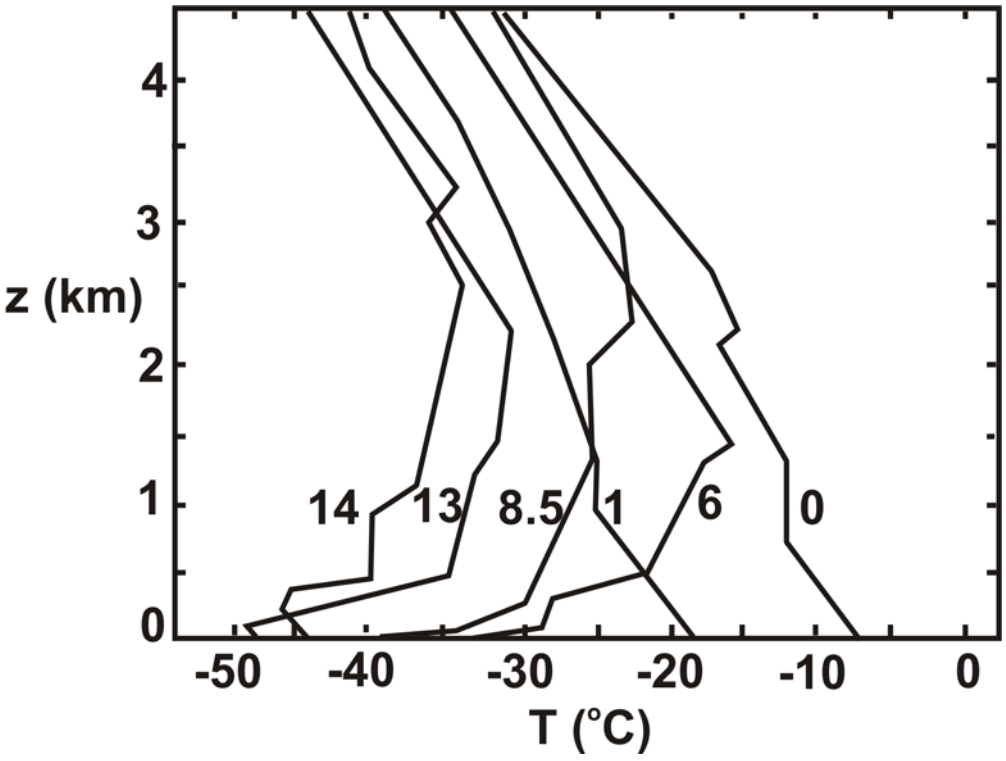

Figure 1

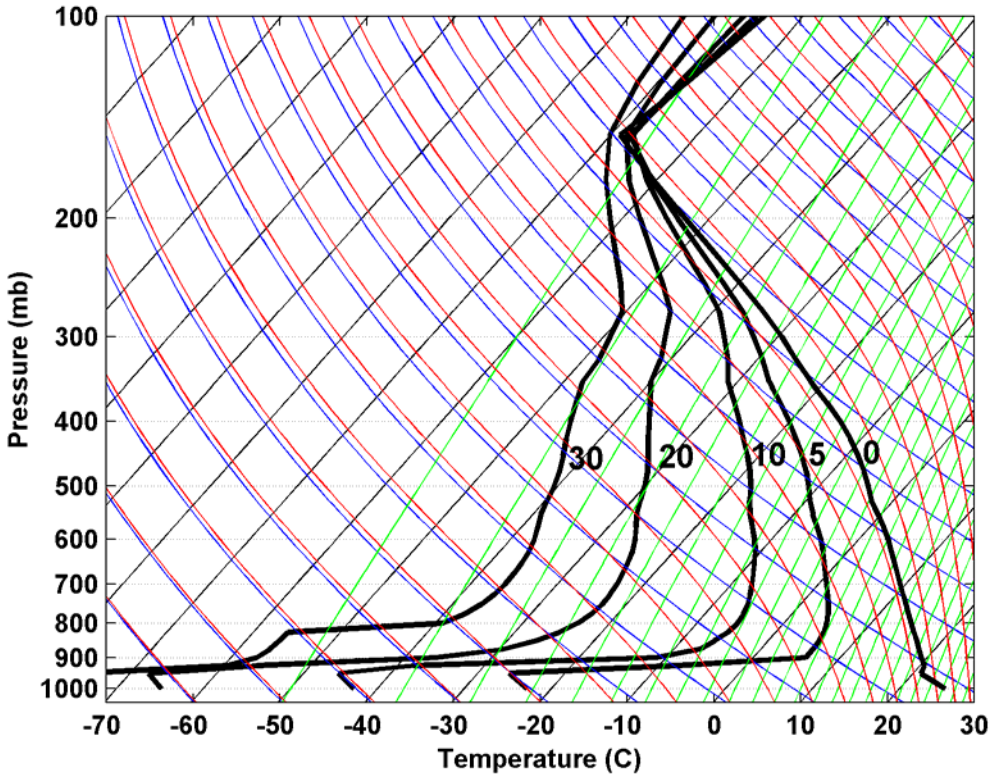
100
200
300
400
500
600
700
800
900
1000
Pressure (mb)
-70
-60
-50
-40
-30
-20
-10
0
10
20
30
Temperature (C)
30
20
10
5
0

Figure 2

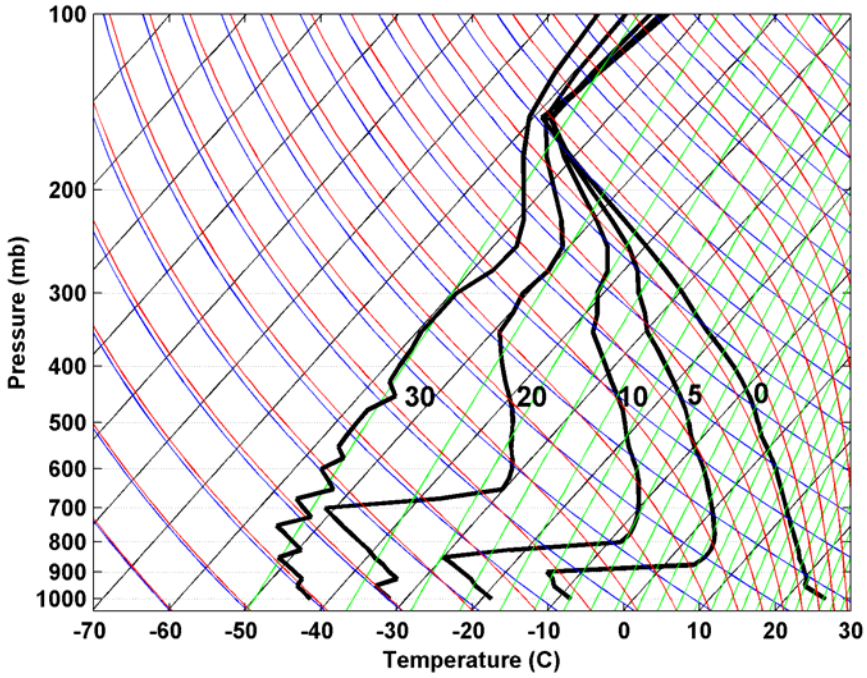

Figure 3a

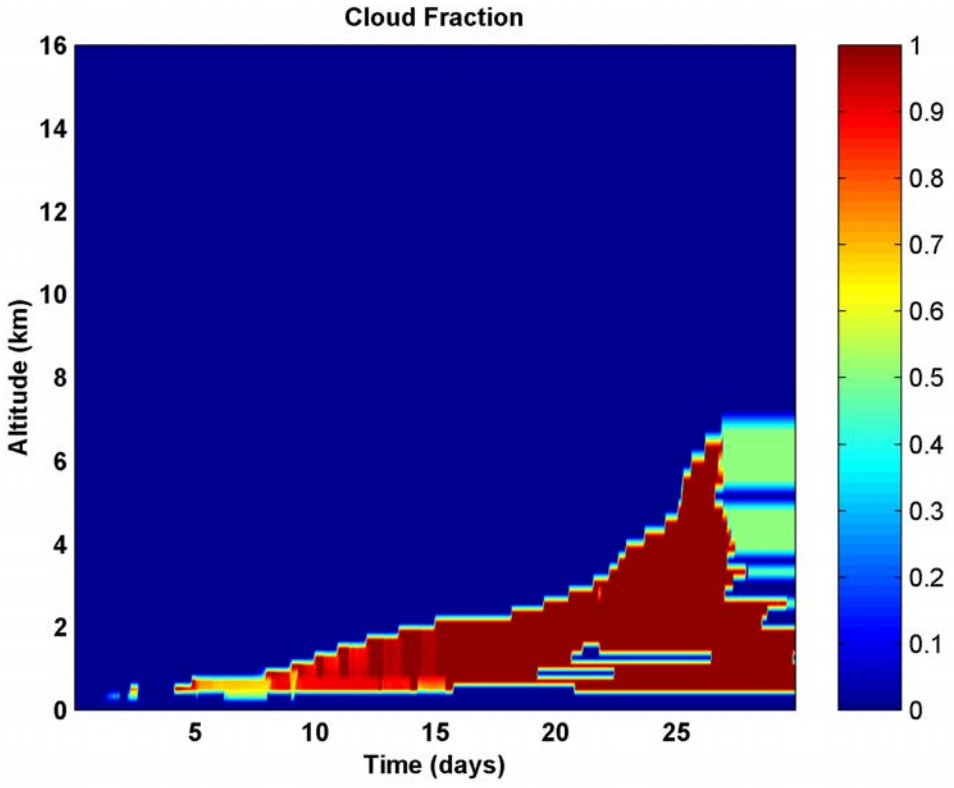

Figure 3b

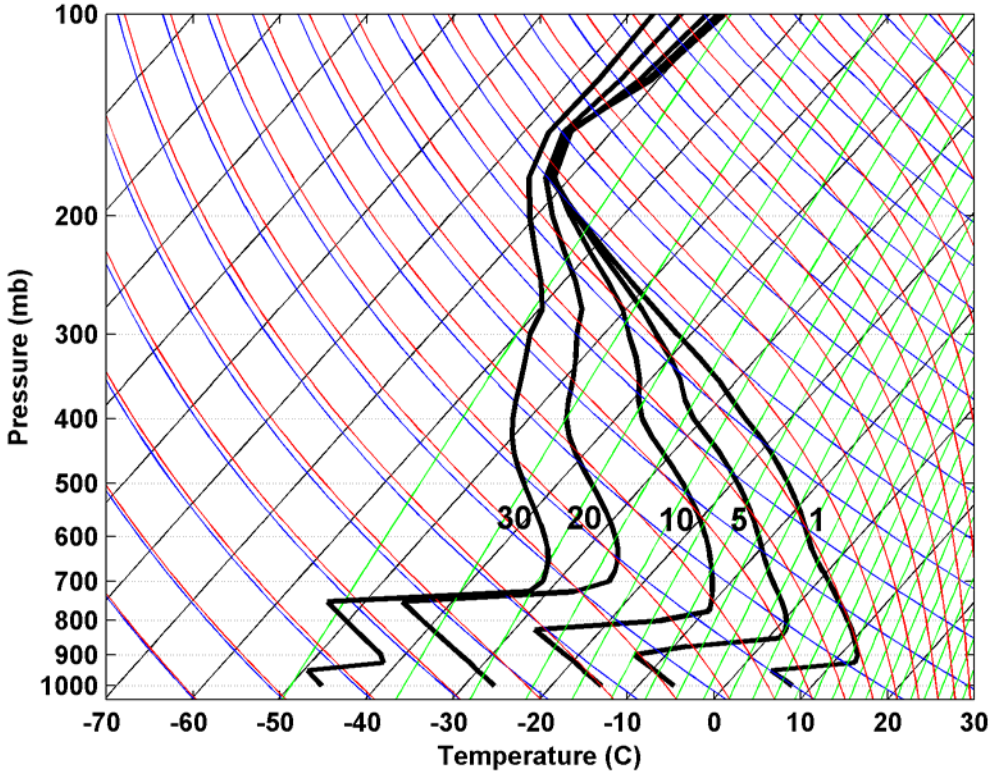
100
200
300
400
500
600
700
800
900
1000
Pressure (mb)
-70
-60
-50
-40
-30
-20
-10
0
10
20
30
Temperature (C)
30
20
10
5
1

Figure 4

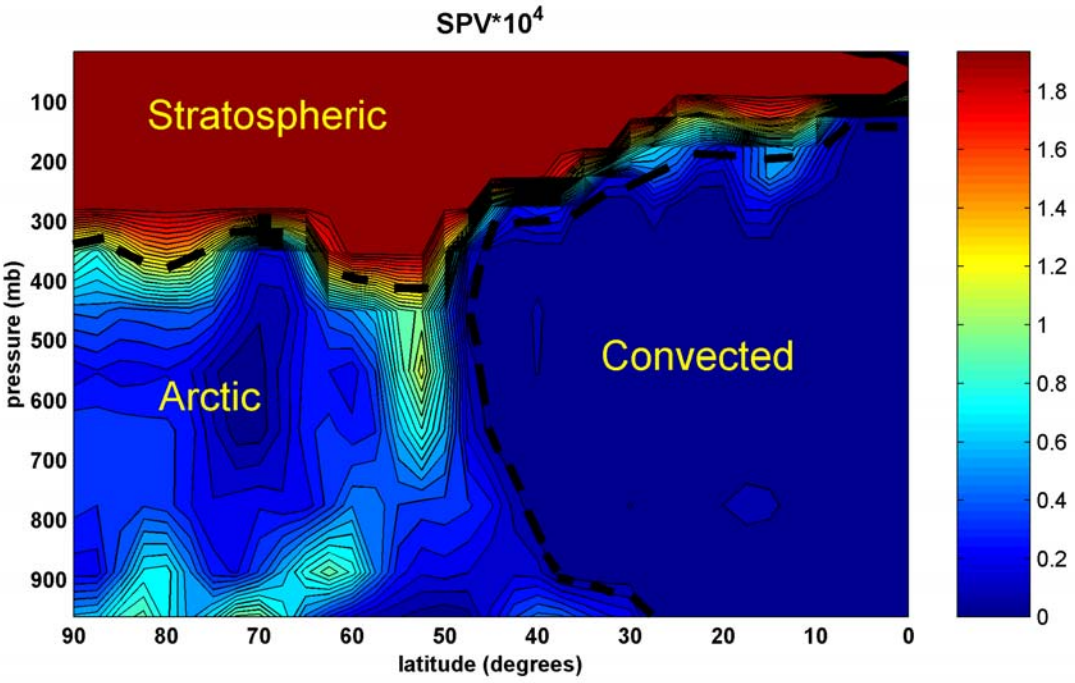
SPV*10^4
Stratospheric
Arctic
Convected
pressure (mb)
100
200
300
400
500
600
700
800
900
90
80
70
60
50
40
30
20
10
0
latitude (degrees)
1.8
1.6
1.4
1.2
1
0.8
0.6
0.4
0.2
0

Figure 5

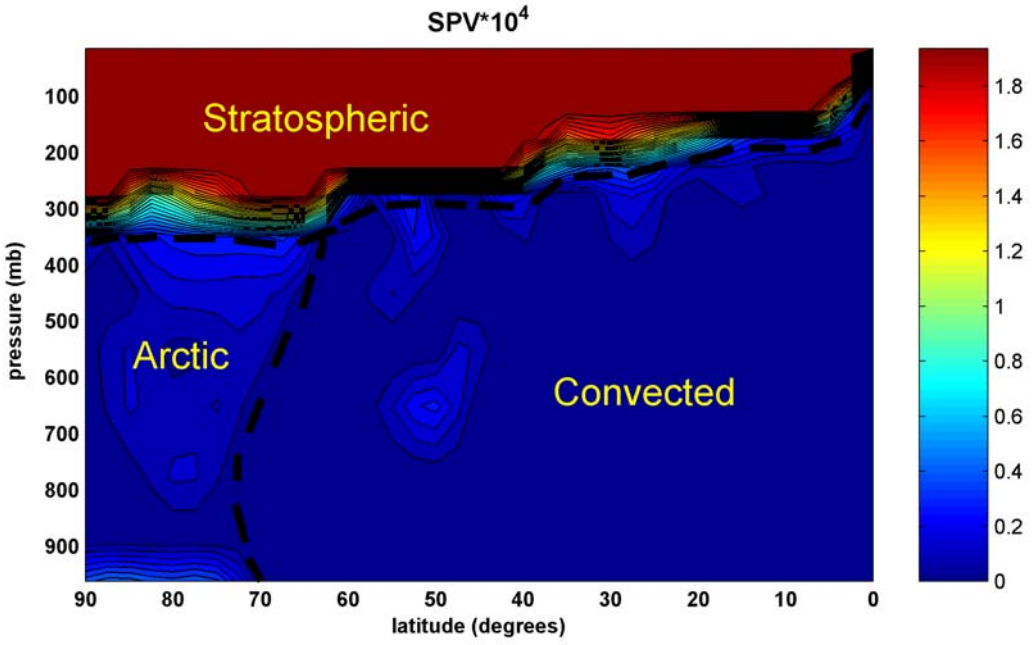
SPV*10^4
Stratospheric
Arctic
Convected
pressure (mb)
100
200
300
400
500
600
700
800
900
90
80
70
60
50
40
30
20
10
0
latitude (degrees)
1.8
1.6
1.4
1.2
1
0.8
0.6
0.4
0.2
0

Figure 6

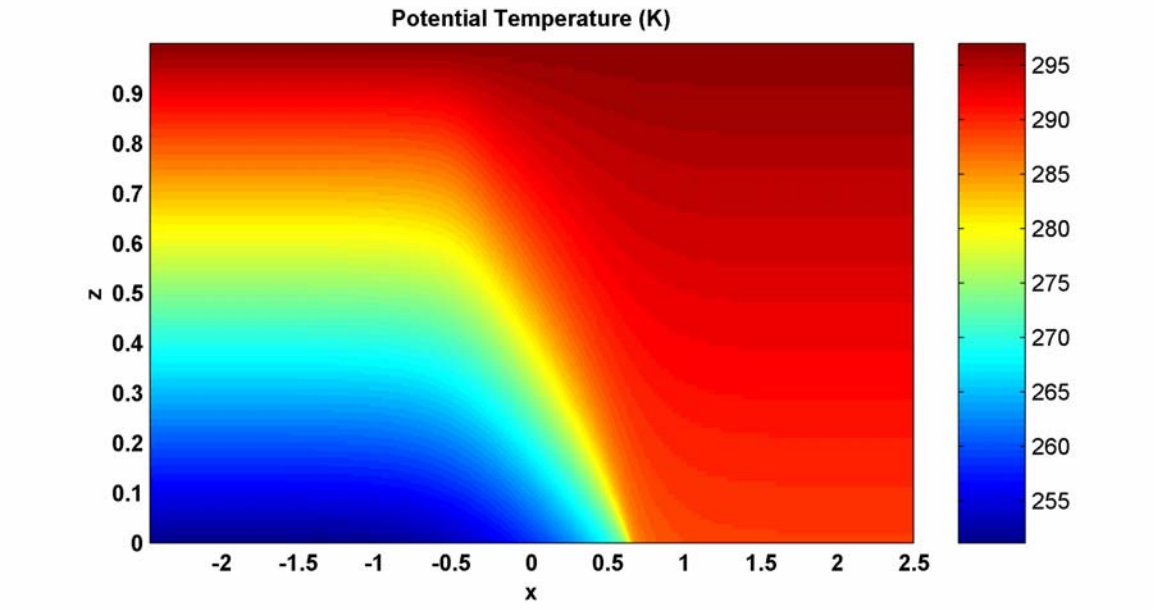

Figure 7a

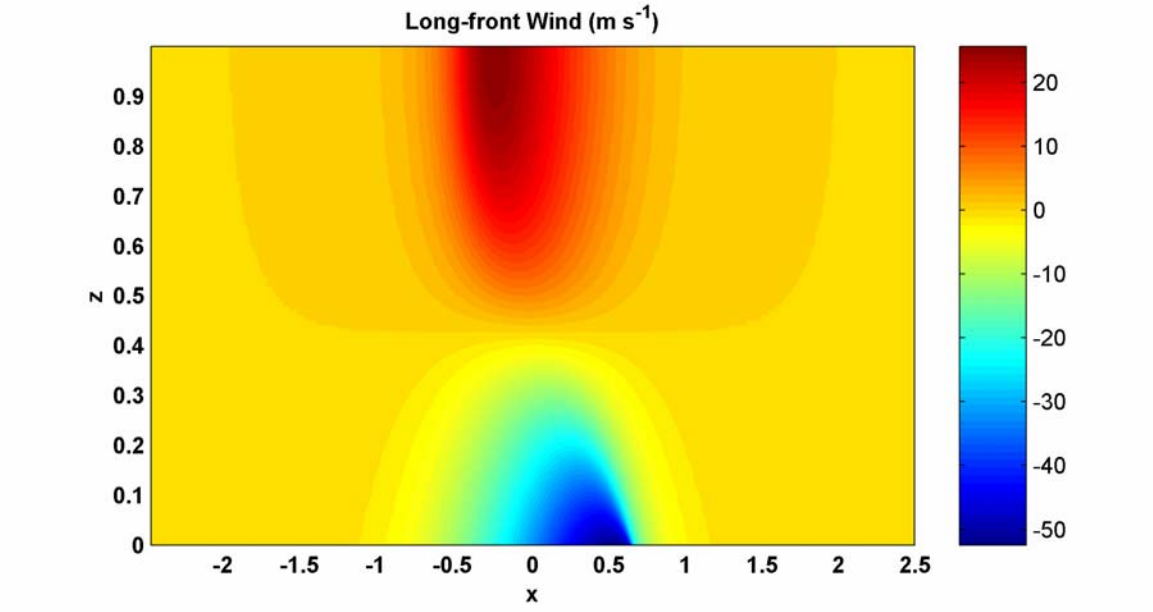

Figure 7b

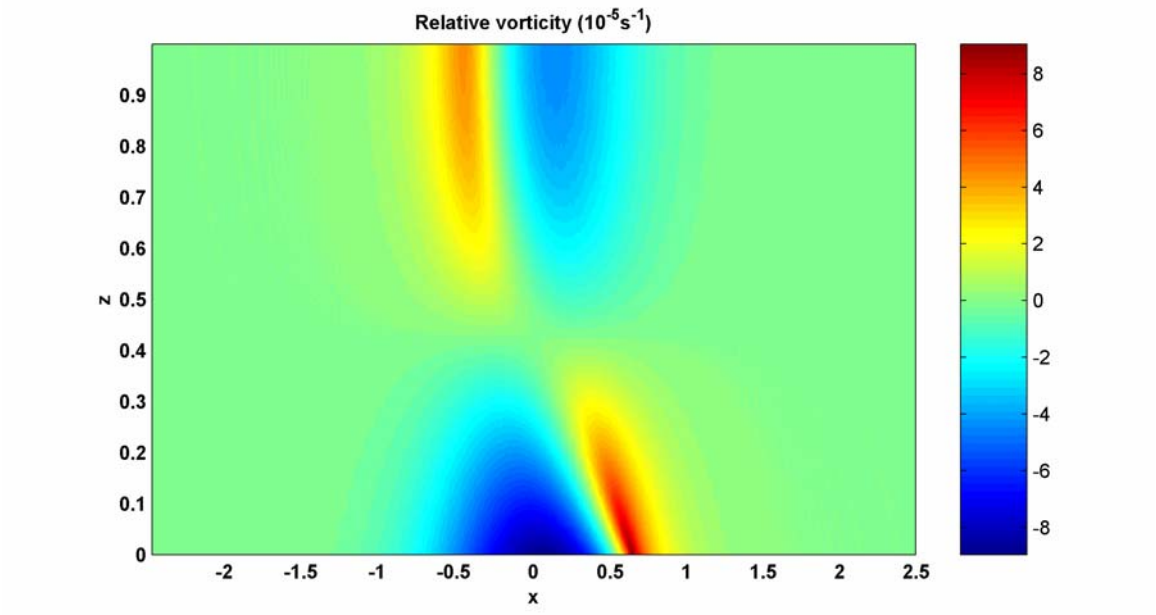

Figure 7c

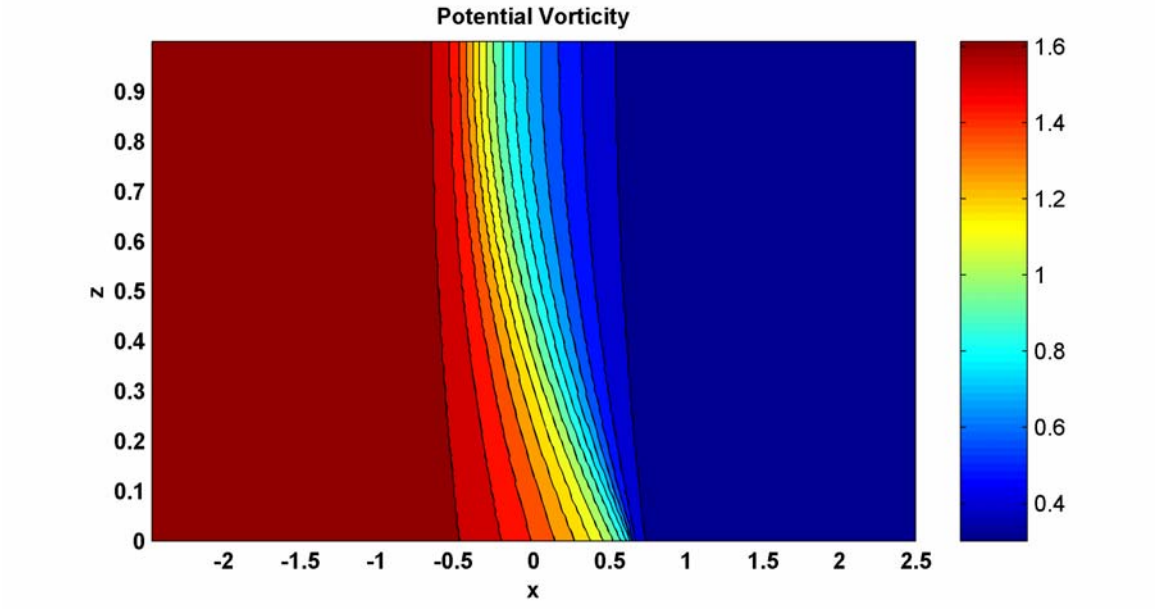

Figure 7d

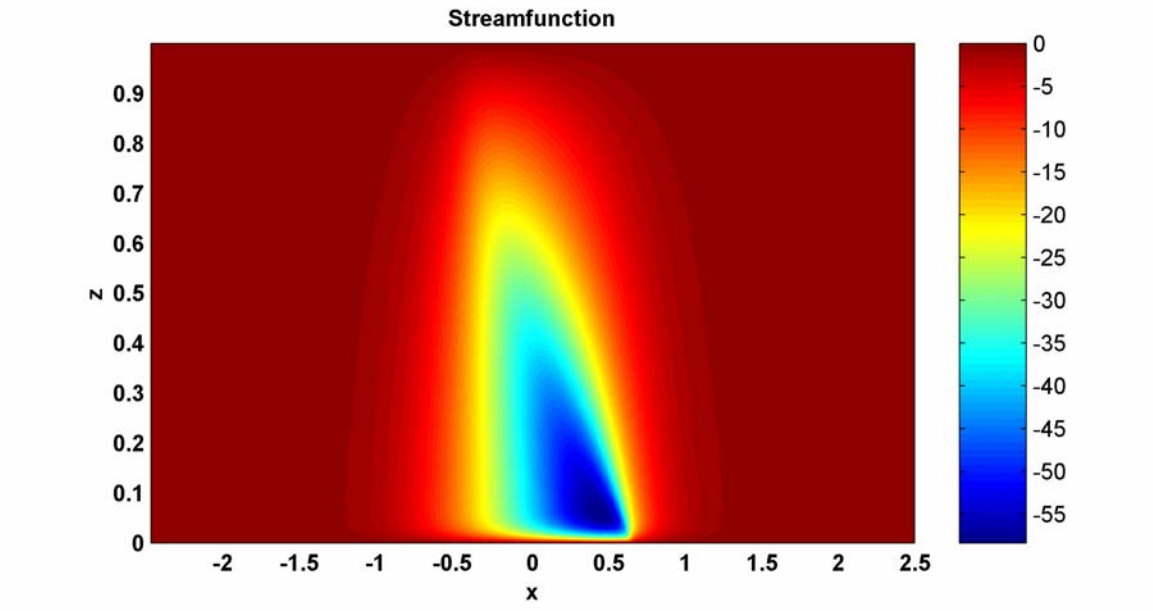

Figure 7e

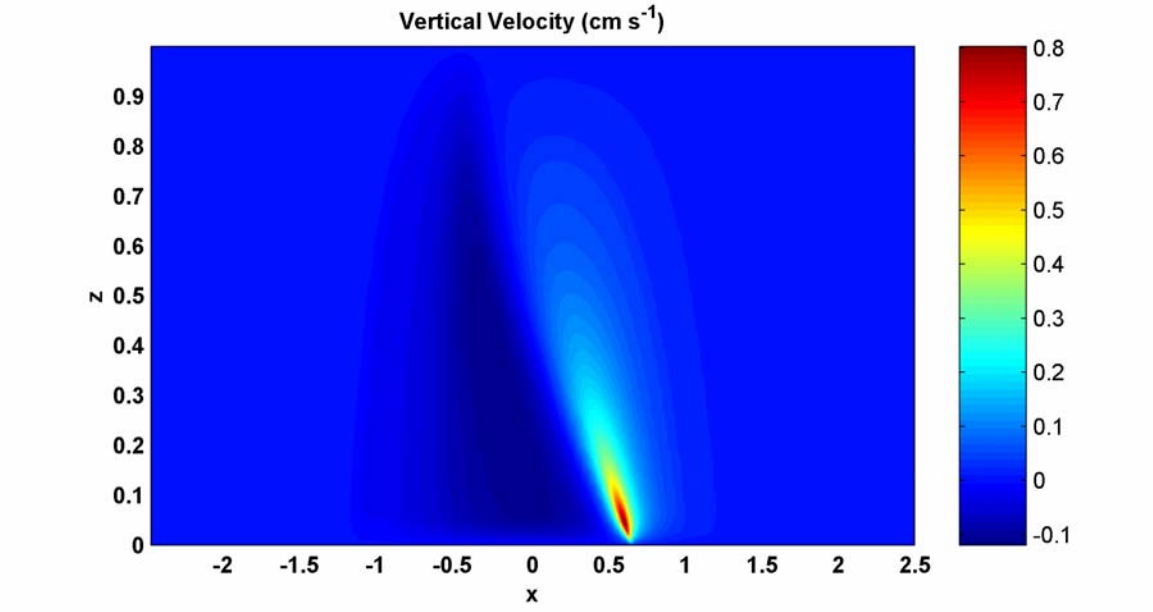

Figure 7f

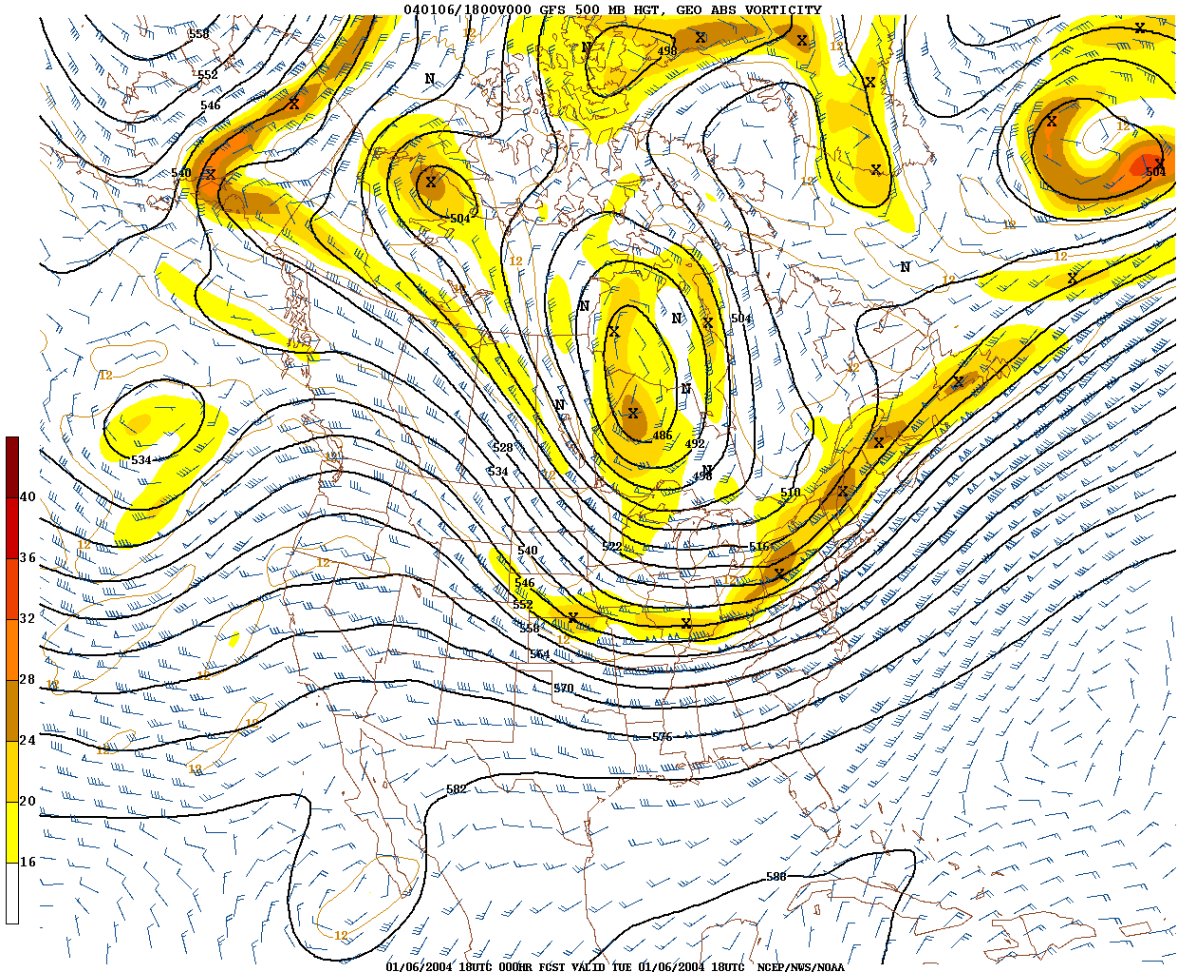
040106/1800V000 GFS 500 MB HGT, GEO ABS VORTICITY
01/06/2004 18UTC 000HR FCST VALID TUE 01/06/2004 18UTC NCEP/NWS/NOAA

Figure 8